Magyarhoni Földtani Társulat
Földtani Közlöny
Hungarian Geological Society

156/3, 323–336., Budapest, 2026

DOI: 10.23928/foldt.kozl.2026.156.3.323

Combustion metamorphic complex in the Miocene coal-bearing sedimentary units of Salgótarján Basin, N Hungary

HORVÁTH, Laura[1,*], WEISZBURG, Tamás[1], PRAKFALVI, Péter[2,3], BIRÓ, Máté[1]

[1]Eötvös Loránd University, Department of Mineralogy, Budapest, Hungary
[2]Novohrad–Nógrád UNESCO Global Geopark
[3]Supervisory Authority of Regulatory Affairs, Budapest, Hungary

*Corresponding author: horvaathl@student.elte.hu
Laura Horváth: https://orcid.org/0009-0004-5784-3217
Tamás Weiszburg: https://orcid.org/0000-0001-8183-4434
Máté Biró: https://orcid.org/0009-0001-5497-6442

Gyulladásos metamorf komplexum a Salgótarjáni-medence kőszéntartalmú üledékes rétegsorában

Összefoglalás

A gyulladásos metamorfózis mint földtani folyamat egyedi metamorf kőzeteket hoz létre, amelyek a sziliciklasztos kontakt metamorf képződményekhez vagy modern kerámiákhoz hasonló tulajdonságokat mutatnak. A kutatási területen, a Salgótarjáni-medence keleti peremén az ipari salakra és kerámiára emlékeztető kőzetek keltették fel a figyelmet. A felszínen kibukkanó kőzetegységek litológiája centiméteres-milliméteres léptékben változik. A legnagyobb mértékű átalakulás az ún. „kéményszerkezetből" származó mintákban figyelhető meg, amelyek nagy hőmérsékletű átalakulásáért a szén égése során felszabaduló gázok elégése a felelős. Ezt a zónát teljesen vagy részlegesen megolvadt kőzetek jellemzik, míg a legkisebb átalakulási fokot a „klinker" metaaleurolit kőzettestek mutatják.

A különböző kőzettípusok ásványtani és szöveti sajátosságainak jellemzésére a terepi megfigyeléseket követően röntgen-pordiffrakciós (XRD) és pásztázó elektronmikroszkópos energiadiszperzív röntgenspektroszkópiai (SEM-EDS) vizsgálatokat végeztünk. Kvarc valamennyi metamorf kőzetben jelen van, többnyire reliktumszemcsék formájában. Minden mintában előfordul plagioklász, ami alapvetően labradoritos-bytownitos összetételű. A klinker kőzetek biotitot, a buchit K-Na-Ca földpátot, piroxént és üveges alapanyagot, míg a paraláva-kőzetek kordieritet, piroxént és földpátot tartalmazhatnak. A klinker minták relikt üledékes szövetet őriztek meg, míg az üveges alapanyagú kőzeteket interszertális szövet jellemzi. A plagioklász gyakran szimplektites kifejlődésű, a piroxén pedig pszeudomorfózák formájában vagy koncentrikus megjelenésű gömbös halmazokként fordul elő. A Salgótarján-Rónabánya melletti feltárás Magyarország első petrográfiailag és ásványtanilag részletesen dokumentált, szálban álló, gyulladásos metamorf komplexuma.

Tárgyszavak: geopark, gyulladásos metamorfózis, buchit, klinker, paraláva

Abstract

Combustion metamorphism as a geological process produces distinctive metamorphosed rocks resembling siliciclastic contact metamorphic formations as well as modern ceramics. Industrial slag and ceramic-looking rocks attracted our interest in our research area, in the eastern part of the Salgótarján Basin, N Hungary. Lithology of the outcropping units varies on centimetre-millimetre scale. The highest degree of alteration was observed on the samples from the "chimney structure", which were annealed by the gases released from the coal burning process. These are characterised by molten or partially molten rocks, while the lowest degree of alteration was in the "clinker" metaaleurolite rock units.

Following field observations X-ray powder diffraction (XRD), scanning electron microscopy with energy dispersive X-ray spectroscopy (SEM-EDS) measurements were carried out on the different rock types to describe the mineralogical and textural characteristics. Quartz is characteristic for all metamorphic rocks, mostly as relict grains. Every sample contains plagioclase which is characterised by labradorite-bytownite composition. Clinker rocks may contain biotite; buchite may contain K-Na-Ca feldspar, pyroxene and glassy matrix; and paralava rocks contain cordierite, pyroxene and feldspar. Clinker samples have a relict sedimentary texture, while rocks with glassy matrix are characterised by intersertal texture. Plagioclase is often symplectitic and pyroxene nodules occur as pseudomorphs or have coccoidal shape. The outcrop near Salgótarján-Rónabánya is the first modern, petrographically and mineralogically well documented in-situ combustion metamorphic complex in Hungary.

Keywords: geopark, combustion metamorphism, buchite, clinker, paralava

Introduction

Pyrometamorphism represents a high-temperature, low-pressure geological process wherein the transformation of original mineral phases is most comparable to the sanidinite facies of contact metamorphism. A prominent sub-type of this phenomenon is combustion metamorphism where sedimentary rocks are altered by the intense heat released during the spontaneous combustion and burning of organic matter – such as coal, bitumen, crude oil, or natural gas – typically operating under near-surface, low-pressure conditions (≤1 kbar) and at elevated temperatures ranging from 550 °C up to 1600 °C (BENTOR et al. 1981, COSCA et al. 1989, HEFFERN & COATES 2004, SOKOL & VOLKOVA 2007). Such combustion events and their associated thermal impacts on sedimentary country rocks are frequently documented worldwide, particularly in connection with major coal-mining districts (SOKOL & VOLKOVA 2007). The ignition of these organic beds can occur via external triggers, such as lightning strikes or wildfires (STRACHER & TAYLOR 2004), or through self-combustion, where the oxidation of organic matter (and subsequently the alteration of pyrite, or other sulphides) increases the internal temperature to the ignition threshold. Spontaneous combustion is further influenced by coal moisture and coal rank (GRAPES 2011).

Once ignited, heat dissipation is primarily driven by convective heat and mass transfer, which propagates vertically through fractures and horizontally via the progressive burning of the coal bed (MISRA & SINGH 1994, HEFFERN & COATES 2004, SOKOL & VOLKOVA 2007, LAITA et al. 2019). However, it is crucial to separate the ignition mechanism from the subsequent burning regime. Spontaneous self-combustion represents the very beginning of the process, after which the system can pass through completely different physicochemical states. In coal fires, the initial, oxygen-poor combustion is often accompanied by intense gas generation and pseudofumarolic activity (SOKOL & VOLKOVA 2007). With adequate oxygen supply, more intense, higher-temperature combustion can develop with extremely steep thermal gradients reaching up to ~140 °C/m within few meters, leading to partial or total melting of the surrounding rocks. Spatially, these different states can even be present simultaneously resulting in different types of rocks, that are characterized by micro-, and macroscale lithological variations. Their mineral paragenesis is dominated by initial moderate-temperature (500-800 °C) dehydration and decarbonation, followed by high temperature (900-1450 °C) metastable melting and rapid mineral reactions, and ultimately by accelerated cooling (SOKOL & VOLKOVA 2007, GRAPES 2011). As temperature rises, the host sedimentary rocks undergo progressive transformation: they form pottery- and ceramic-like clinkers, partially melted buchites, and ultimately, completely melted paralavas that crystallize and quench within the so called "chimney structures" (HEFFERN & COATES 2004, GRAPES 2011).

While massive combustion metamorphic complexes are known globally – such as the Powder River Basin in North America, which spans over 500,000 km^2 (BENTOR et al. 1981, COSCA et al. 1989), and the exotic, mineral-rich Hatrurim Basin in Israel, which is a paradise for rare mineral species (GROSS 1977) – they also occur in deep settings. In Central Europe, combustion metamorphic rocks can be found even at depths of 780–870 meters in the Upper Silesian Coal Basin of Poland, where normal faulting in an extensional regime and the exhumation of coal seams to depths of 100–150 meters historically facilitated ignition (NAWROCKI et al. 2022). Furthermore, the Most Basin in the Czech Republic represents a relevant natural analogue within Central Europe, where the natural combustion of Tertiary coal seams generated extensive pyrometamorphic rocks (covering ~1400 km^2), primarily sintered clays known as porcellanites, as well as Fe-Mg-Ca-rich buchites and paralavas (ŽÁČEK et al. 2005, 2015). These Pliocene age fires reached temperatures exceeding 1150 °C and provide insights into long-term, natural combustion metamorphic systems (ŽÁČEK et al. 2015).

In addition to these natural occurrences, burning coal-mine dumps in Central Europe, such as those in Poland and the Czech Republic, can serve as relevant process analogues (CIESIELCZUK et al. 2015a, 2015b; ŽÁČEK & SKÁLA 2015). Although they are anthropogenic, are also crucial for studying spontaneous combustion in detail (e.g., temperature gradients, melt formation). For instance, investigations from the Wojkowice coal-waste dump have demonstrated a clear spatial zonation, transitioning from a central zone characterized by paralava and scoria, to a hematite-bearing thermal aureole, and finally to an unaltered external zone (CIESIELCZUK et al. 2015a). Furthermore, the study highlights that the extent of pyrometamorphic alteration is governed not only by peak temperatures, but also by the initial protolith composition, rock grain size, and the dynamics of oxygen supply.

This study presents the first modern, petrographically and mineralogically detailed characterization of the newly identified Rónabánya Combustion Metamorphic Complex (RCMC), found in the layers of the Salgótarján Brown Coal Formation, in the Salgótarján Basin, N Hungary (Central Europe). In the context of Hungary, pyrometamorphic occurrences related to coal fires in the Salgótarján Basin must also be mentioned, such as the thermally altered waste dump of the Károly Shaft (SZABÓ et al. 2025). Although its depositional setting and evolution differ from the in-situ, natural system presented in this study, it can provide a vital comparative context.

Geological background: Rónabánya and the Salgótarján Basin

The Salgótarján Basin, located in N Hungary, Central Europe, is historically famous for its natural coal-burning "craters," with documented natural coal fires burning for several months as early as the 18th century (JENEI 1968). Despite a rich history of industrial-scale brown coal mining since 1848 (NOSZKY 1931) and repeated reports of underground combustion events during excavation (DZSIDA 1944), an extensive combustion metamorphic rock suite had not yet been comprehensively described in the area. Geologically,

the basin is filled with Paleogene and Neogene sedimentary units that locally exceed 3,000 meters in thickness. These include Upper Oligocene "glauconite sandstones" and Pecten-bearing shallow marine sandstones, overlain by continental mudstones (KERCSMÁR & BUDAI 2015). This sequence is discordantly succeeded by the ~17 Ma Tihamér Rhyolite Lapilli Tuff Formation (LUKÁCS et al. 2018), which serves as the base for the Salgótarján Brown Coal Formation (RADÓCZ et al. 2023).

Near Rónabánya, our field of study in the Salgótarján Basin, only the limnic, III. main coal seam is preserved, measuring 4 to 4.4 meters in thickness and dipping near-horizontally. This seam is split into lower and upper bed by an interbedding shale or sandy-siltstone layer (NOSZKY 1931). The siliciclastic host rock frequently contains silicified or carbonized plant remains (RADÓCZ et al. 2023). This sedimentary sequence is structurally undisturbed, except for the crosscutting Pliocene basaltic volcanism (the Salgóvár Basalt Formation). The heat from these basaltic pipes coked and purified the coal only on a decimeter scale, without forming significant contact metamorphic aureoles in the Miocene sediments (based on the personal communication of P. PRAKFALVI). Prior erosion removed the upper portion of the Salgótarján Brown Coal Formation, while the basalt practically covered, and protected these underlying layers, enabling intensive coal mining in the 19th and 20th centuries (NOSZKY 1931). The overlaying basalt is apparently absent from the immediate metamorphic sequence, leaving it unresolved whether the Szilvás-kő lava flow ever reached this specific area or was subsequently eroded away. Recent geomorphology is mostly dominated by erosion, where the combustion metamorphic units are selectively denudated on a high angle slope.

Samples and Methods

Samples

Sampling was performed at two sites, using both a raster-based and a texture-based approach. Texture-based sampling was performed to identify the characteristic rock types throughout the complex and gain appropriate samples for petrographic descriptions. Raster-based approach was used to estimate the extent of metamorphic halo around the combustion centre. Thus, the thermal alteration through the complex could be followed. From the samples collected by the textural approach 30 µm polished thin sections were made for transmitted and reflected light petrography and for SEM-EDS measurements. Samples from both approaches were grinded within agate mortar for XRD measurements.

Methods

Microscopy was performed using a Zeiss Axioplan polarised light petrographic microscope equipped with Zeiss Axiocam 208 4K mounted camera. Ratios of rock forming constituents were counted in volumetric% by the line counting method. XRD analyses were implemented with a Siemens D5000 X-ray diffractometer equipped with θ-θ geometry (Bragg-Brentano) goniometer using a Cu X-ray source with a K-α= 1,5406 Å, K-β being filtered by secondary graphite monochromator. The results of the measurements are found in Supplementary Material 1A. For semi-quantitative mineral and whole rock compositional measurements an AMRAY 1830i scanning electron microscope was used equipped with EDAX PV9800 energy dispersive detector. SEM-EDS measurements were carried out using 20 kV acceleration voltage and 1nA sample current each. The SEM-EDS was calibrated using Microspec silicate reference materials. Whole rock compositional measurements were made on 100x100µm fields with unfocused electron beam scanning for 100s time. The results of the measurements are found in Supplementary Material 1B.

Results

The outcrops

Located on the steep northern hillsides of Szilvás-kő near the Gusztáv IV adit at Rónabánya, the first outcrops of the metamorphosed rocks are found at coordinates N 48°07.429', E 019°53.768'. The RCMC exhibits a horizontal exposure of approximately 400 meters in an E-W direction and a vertical thickness of 10 meters along the steep, 30-meter-high valley wall. Stratigraphically, the complex sits above the lower bed of the III. main coal seam, having formed from the combustion of the upper coal bed and its overlying sediments. The resulting rock formations are highly heterogeneous at both macroscopic and microscopic scales, with protolith siltstone (aleurolite), metasiltstone (metaaleurolite), buchite, and paralava frequently alternating within a single meter. Under present-day geomorphological conditions, these combustion metamorphic units are selectively denuded on the high-angle slope.

The combustion metamorphic rocks were studied in two well preserved sites: one site (S1, *Fig. 1a, Fig. 2*) is associated with the entrance of the underground mining site at Gusztáv IV. adit and the other site (S2, *Fig. 1b, Fig. 2*) is ~70 m East from the first unit with no known connection to modern day mining activities. However, fragments of clinker and buchite were also found in slump sediments 200 m NW from the above-mentioned outcrops, hence the real extent of the combustion metamorphic complex is yet to be determined. The hillside near the first unit has an average 30° slope angle but in the unaltered units it can reach up to 50°. Metamorphosed rocks within the units can vary locally on a centimetre-millimetre scale (*Fig. 3*). In the S1 unit, which stands out in the outcrop morphologically as a chimney structure, the altered sedimentary strata are over 20 m wide and 12 m high and circularly surrounds the Gusztáv IV. entrance. The inner part of this chimney structure is built up by heavily fractured, brecciated red and grey clinker and buchite clasts

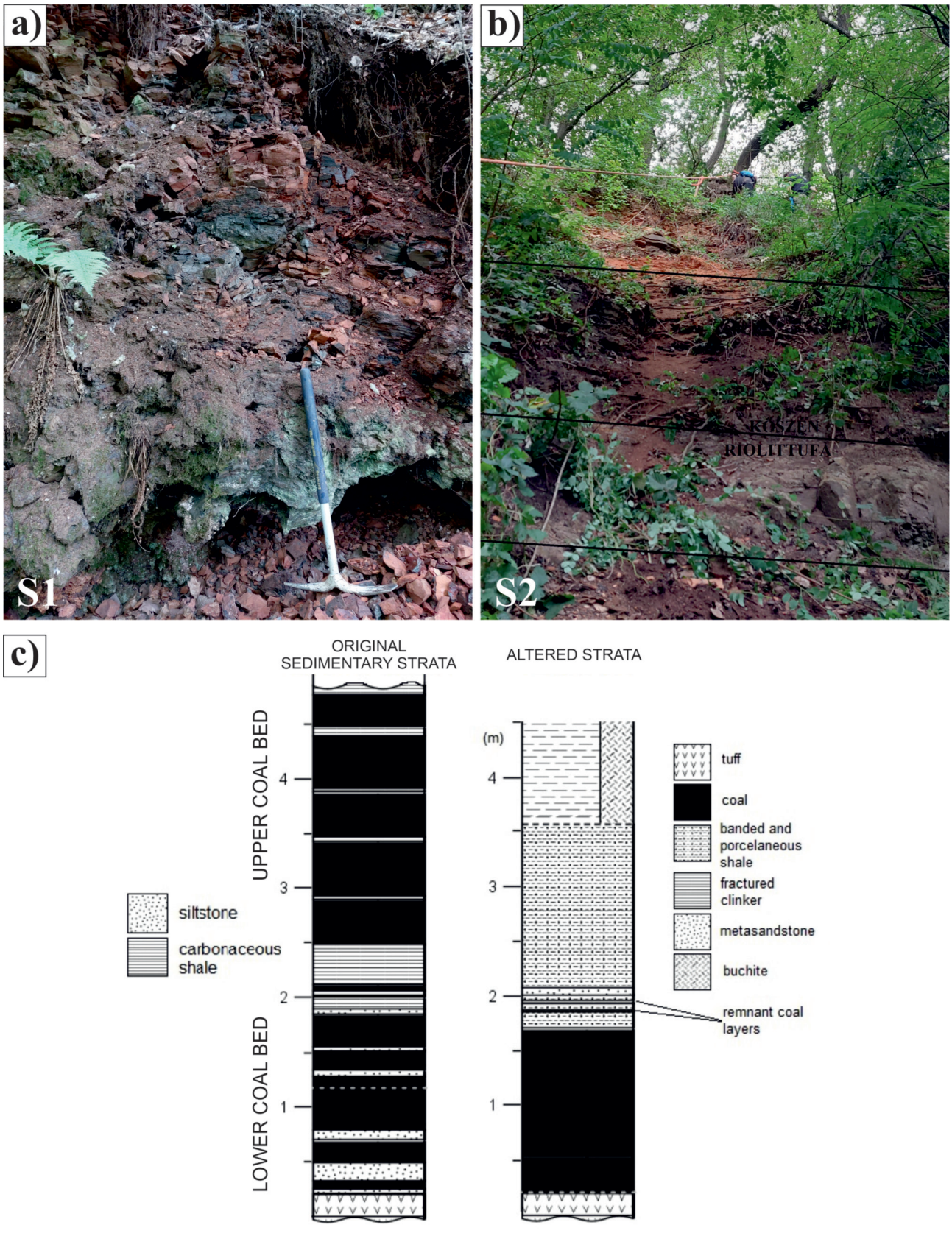


Figure 1. The Rónabánya Combustion Metamorphic Complex (RCMC): a) the chimney structure (S1 outcrop) on the field; b) the altered rocks on the steep hillside (S2 outcrop); and c) a comparative diagram of the original sedimentary strata of the 3rd coal seam (Salgótarján Brown Coal Formation) and the altered strata from the S2 outcrop

1. ábra. *A Rónabánya Gyulladásos Metamorf Komplexum (RGMK). a) kémény struktúrája (S1 feltárás) terepen; b) átalakult kőzetei a meredek domboldalban (S2 feltárás); és c) a Salgótarjáni Barnakőszén Formáció 3. széntelepének eredeti üledékes rétegsorának és az S2 feltárás átalakult kőzetekből álló rétegsorának összehasonlító ábrája*

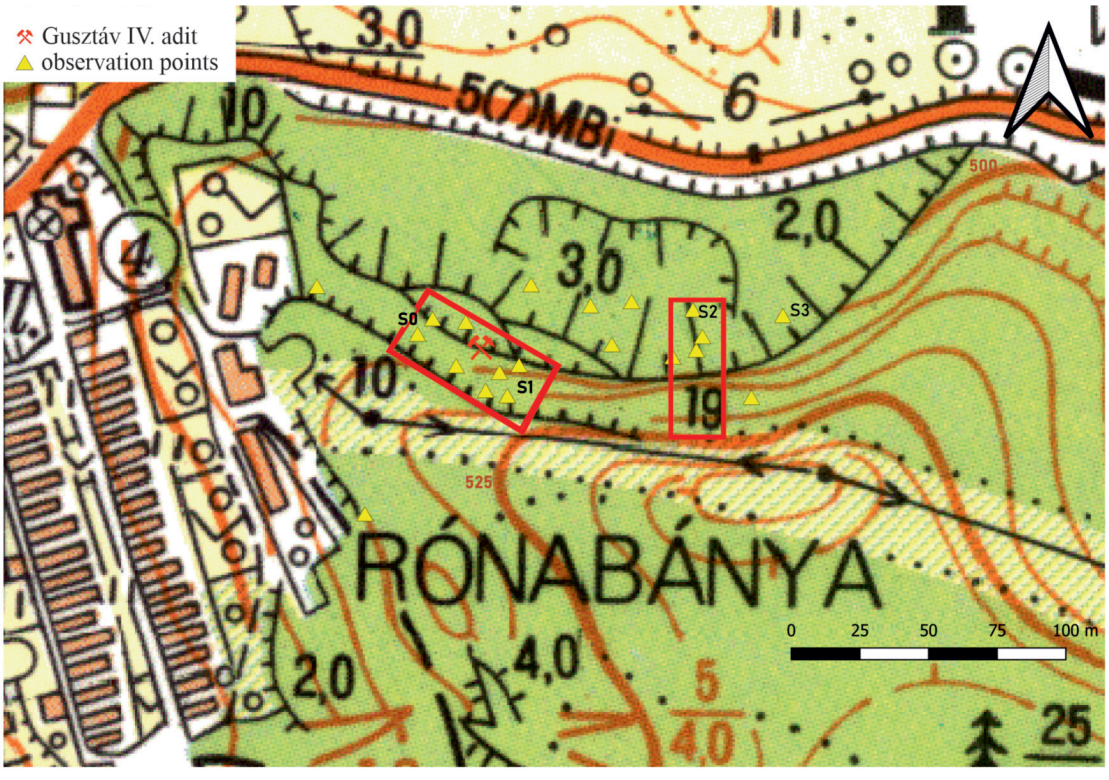


Figure 2. Topographic map view of the outcrops (S1 and S2) in the Rónabánya Combustion Metamorphic Complex with the entrance of Gustav IV. adit and the marked observation points made during fieldwork

2. ábra. *A Rónabánya Gyulladásos Metamorf Komplexum feltárásainak (S1 és S2) elhelyezkedése domborzati térképen a Gusztáv IV. táró bejáratával és a terepen tett észlelések pontos helyével*

cemented by dark, lustrous and vesicular paralava (*Fig. 3e-f*). The brecciated rocks have a gradual transition to less altered buchite (*Fig. 3c-d*) and clinkers (*Fig. 3b*) towards the distal outcrops of the complex. Selective denudation resulted that the more resilient brecciated units stand out of the outcrop. Lower grade clinkers are usually characterised by more intensive erosion and up to 40 cm thick soil formation. Moving further away from the chimney structure at S1 unit, the grade of the alteration tends to decrease to the point where unaltered sedimentary rocks - the protolith - can be found (*Fig. 3a*). In the S2 unit the Tihamér Rhyolite Lapilli Tuff Formation is overlain by a 1,9 m thick coal layer continued by the altered sedimentary strata made up of pseudoconform clinker, metasandstone and buchite (*Fig. 1b, 1c*).

Petrography

Protolith

The yellowish-brown, micaceous, fine laminated, sandy aleurolite contains unoriented carbonaceous platelets along the bedding planes. The amount of these platelets does not exceed 2% for the whole rock although it may occur in rock-forming amounts along some planes. The mineral composition of the protolith is typical for siltstones: quartz, smectite, 10 Å phyllosilicate (biotite/muscovite), chlorite and Na-plagioclase (Suppl. 1A. and 1B.). The presence of carbonates as detrital grains – Mg-calcite and dolomite – is verified too. Accessory minerals of the protolith are zircon, xenotime, apatite and spessartite. Apart from mica, the minerals are distributed in the rock without any noticeable orientation, with an average grain size of 30-50 μm. The rock is cemented by a multiphase, complex Fe-oxide and SiO_2 mixed cement. Gypsum was also noted as a secondary mineral.

Clinker

The most commonly occurring rocks in the complex are the least recrystallised, annealed and thermally altered, yellow to red sometimes even black coloured metaaleurolites: clinkers. The mineral assemblage of these ceramic-like metaaleurolites is dominated by quartz and feldspar: the less altered samples are built mainly from quartz, Na-plagioclase, 10 Å phyllosilicate (mica), and hematite with minor amphibole, with accessory minerals like ilmenite, zircon, monazite, xenotime, and apatite (Suppl. 1A. and 1B.). With increasing alteration grade, the relative quantity of quartz and 10 Å phyllosilicate tends to decrease, while cristobalite and clinopyroxene (augite-diopside) appear. Most of the metaaleurolites are showing relict sedimentary, blastoclastic texture (*Fig. 4a*), but increasing alteration grade results in a more packed, ceramic-like texture. Glass (with heterogeneous composition) and opaque minerals like ilmenite are present replacing original mineral phases such as biotite. Idiomorphic, 1-5 μm enstatite crystallites are generally grouped into 20 μm zoned nodules – as pseudomorphs – with augitic

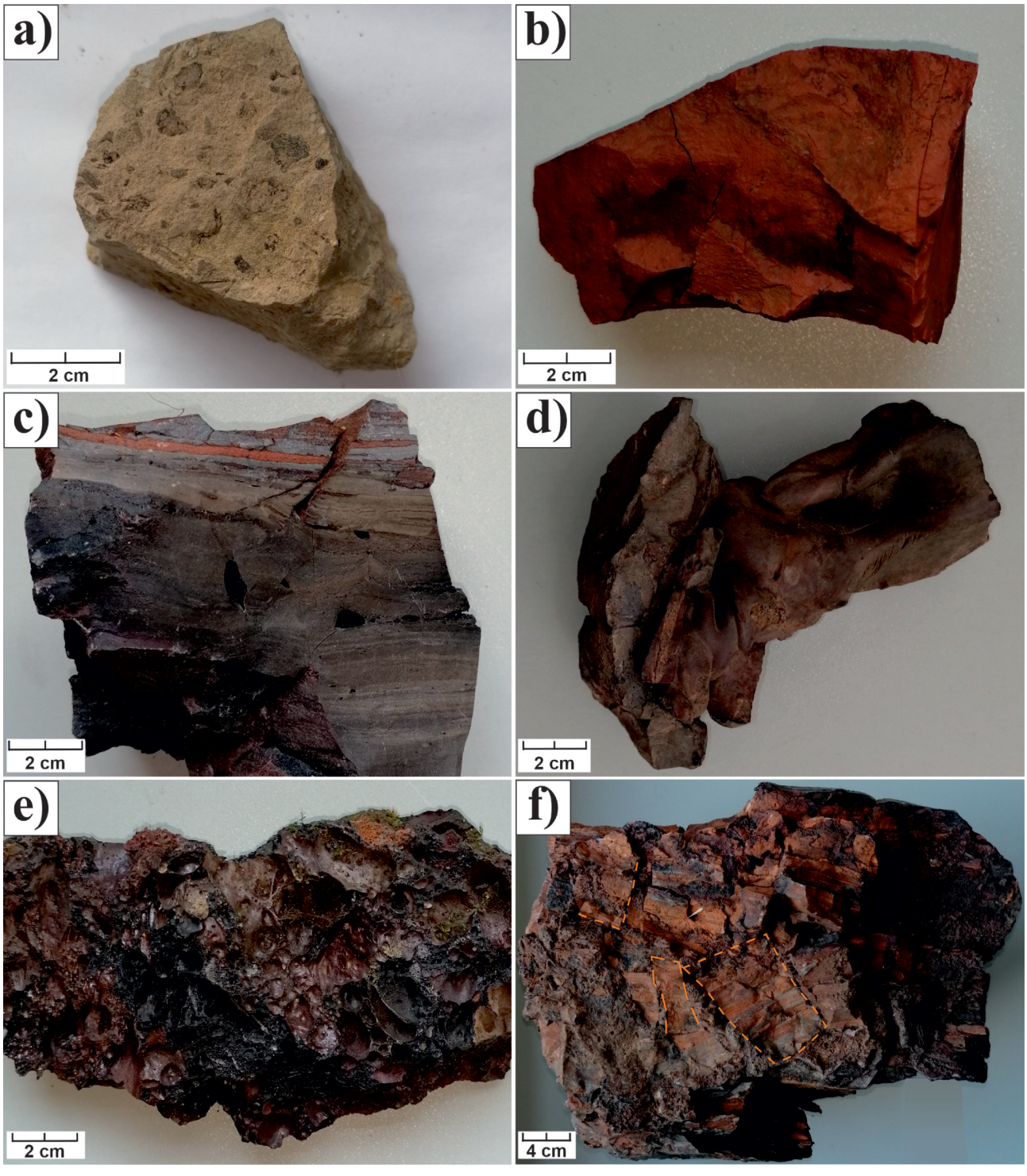


Figure 3. Photographs of the rocks of the Rónabánya Combustion Metamorphic Complex: a) The protolith – yellow aleurolite with remnants of carbonaceous plant fragments; b) Red metaaleurolite – clinker – with remnants of original sedimentary layering and homogeneous brick-red colour; c) Cut surface of glassy pseudoconform buchite with alternating red-gray-black layers, seemingly preserving the original sedimentary layering. The observed lamination is disrupted by microscale fractures, faults, and convoluted lamination possibly related to gas escape; d) Pāhoehoe-like paralava flow; e) Slag-like foamy paralava with glass-covered slightly elongated bubbles; f) metaaleurolite-buchite breccia (clasts highlighted) cemented by slag like paralava – typical facies for the chimney structure

3. ábra. *A Rónabányai Gyulladásos Metamorf Komplexum kőzeteinek fényképei: a) A protolit – sárga aleurolit szenesedett növénymaradványokkal; b) Vörös metaaleurolit (klinker) az eredeti üledékes rétegződés nyomaival és homogén téglavörös színnel; c) Üveges, látszólag konkordáns (pszeudokonform) buchit vágott felülete váltakozó vörös-szürke-fekete sávokkal, amelyek látszólag megőrizték az eredeti üledékes rétegződést. A megfigyelt laminációt mikroméretű repedések, vetők és gázszökés okozta konvolúciók (fodrozódások) szakítják meg; d) Pāhoehoe-jellegű (kötélláva típusú) paralávafolyás; e) Salakszerű, habos paraláva üveges bevonatú, enyhén megnyúlt hólyagüregekkel; f) Metaaleurolit-buchit breccsa (klasztok kiemelve) salakszerű paralávával cementálva – a kéményszerkezet tipikus fáciese*

rims. (*Fig. 4b*). The cavities are often shaped of perimorphs, but elongated vesicles are common too, parallel to the relict lamination.

Buchite

Buchite samples from the outcrops are reddish-brown in colour with grey and black nodules and bands appearing in layers. These bands vary in thickness from 1 mm to 2 cm often undulating or showing maze-like structures. Visible mineral phases cannot be macroscopically distinguished; the rock's texture is aphanitic. The rocks are porous along the grey bands, with elongated, almost flattened cavities 50-100 μm in size. Pentagonal to hexagonal columnar features are visible on the margins of some samples, similar to cooling cracks, with hairline cracks penetrating vertically into the rock to a depth of ~1 cm. In all the buchite samples, an elevated background (between 15-35° θ angles) - characteristic of amorphous materials - is clearly detectable (Suppl. 1A.). Main mineral phases are quartz, cristobalite+tridymite, plagioclase and enstatite (or more generally orthopyroxene) (Suppl. 1A. and 1B.). Overall, the texture of the samples is characterised by more than 10 v% glass, with idiomorphic, hypidiomorphic crystals "floating" in the glassy material, thereupon the texture is hyalopilitic (*Fig. 4c-d*). However, original sedimentary texture may still be recognisable by the presence of oriented relict quartz grains. However, there are domains where the minerals contact, these domains can be considered intersertal (*Fig. 4e*). The rocks typically contain 20-25 v% resorbed, round-edged, fractured quartz grains; approximately 20% rosette-like or pseudomorphic pyroxene (enstatite core with augite-diopside rim); and 15-20% skeletal, symplectitic, or needle-like plagioclase (*Fig. 4e*), with tabular cristobalite floating in the glassy matrix or being intergrown with skeletal plagioclase. A concentric expansion crack system is frequently observed in the K-Al rich glass surrounding the detrital quartz grains showing an onion-shell like pattern. Ilmenite occurs in association with the pyroxene nodules or in smaller lone aggregates. In addition, zircon and Ca-phosphate were identified as accessory minerals.

Paralava

The paralava rocks occur in significant amount in the chimney structure at the Gustav IV. adit. Within the chimney structure, cracks and fissures of up to several metres in size can be observed. Besides the pure slag-like paralva rocks the most abundant facies in the chimney structure is the brecciated metaaleurolite (both buchite and clinker) cemented with paralava.

The rocks are black, grey or red coloured, and extremely vesicular. The surface of cavities is generally characterised by a vitreous lustre, with an earthy appearance on weathered surfaces. A major difference between the red and black paralava is in the shape of the cavities: black bands tend to have rounded and flattened vugs while red parts of the same rock show cavities with irregular, angular shapes. The size of cavities in the paralava cementing the breccias in the chimney structure varies from 80 μm to 4 mm with a bimodal size distribution. Paralava slags, without significant juvenile clasts are usually either characterised with cavities ranging from 2-40 mm in size. The walls of the cavities are coated with reddish, sometimes greyish glass. Fragments of torn up clinker clasts may be embedded in the smooth surface of the rocks. Similarly to buchites, the rock does not contain any visible mineral grains, thus the macroscopic texture is aphanitic.

The mineral composition of the samples is similar to the buchites: SiO_2 polymorph crystals – cristobalite+tridymite, plagioclase, K-Na-Ca feldspar and Fe-Ti oxides are present with cordierite as a main component besides the (mostly detrital) quartz (Suppl. 1A. and 1B.). The rocks contain fragmented detrital quartz and resorbed remnants of feldspar in the glassy material, in an amount of about 30 v%. Clumps of ilmenite and iron-oxide rims surround skeletal plagioclase crystals, while cordierite, cristobalite and glass were observed in patches with an intersertal texture (*Fig. 4f*). The observed patches are rimmed by opaque minerals, and contain approximately 50% plagioclase, 15-20% cordierite, and an indeterminable proportion of cristobalite in glassy matrix. In addition, the vitreous matrix of the rocks contains needle-like, 10-40 μm, sometimes twinned Ca-rich plagioclase. The intersertal texture is supported by plagioclase skeletal crystals, while cristobalite is showing triple joints with the tabular-isometric crystals of cordierite in the mesh of the plagioclase needles (*Fig. 4f*).

Discussion

Zonal distribution of pyrometamorphic facies

The RCMC reveals a zonal distribution of pyrometamorphic facies. The outcrop at Gusztáv IV. adit shows the vertical cross-section of a chimney structure, which is possibly the highest temperature zone of the outcropping metamorphosed assemblage (Sokol & Volkova 2007). The pseudoconform buchites without paralava surround the chimney structure, while the outermost zone is made of "clinker" metaaleurolite rocks, which are present in the largest volume. This distributional trend suggests a thermal zonation around the chimney structure. In the S2 outcrop the slag-like paralava rocks only occur in the debris and no chimney structure is detected on the surface. This could be the outcrop of a discrete distal development of an already eroded-down chimney-structure or a unit of the complex where a brecciated chimney structure failed to develop. The relationship between the above-mentioned three types of rocks is best observable on a centimetre scale. The buchite, which is usually associated with fractures, is related with clinker units in a gradual transition, and paralava rocks with a stalactite-like appearance are also usually present in the fractures of buchite. However, the paralava rocks are typically observed in lenticular development between two metaaleurolite layers. Brecciated metaaleurolite clasts cemented by paralava are present in the chimney structure in S1 outcrop. Moving upwards in this outcrop, the paralava cement disappears after a

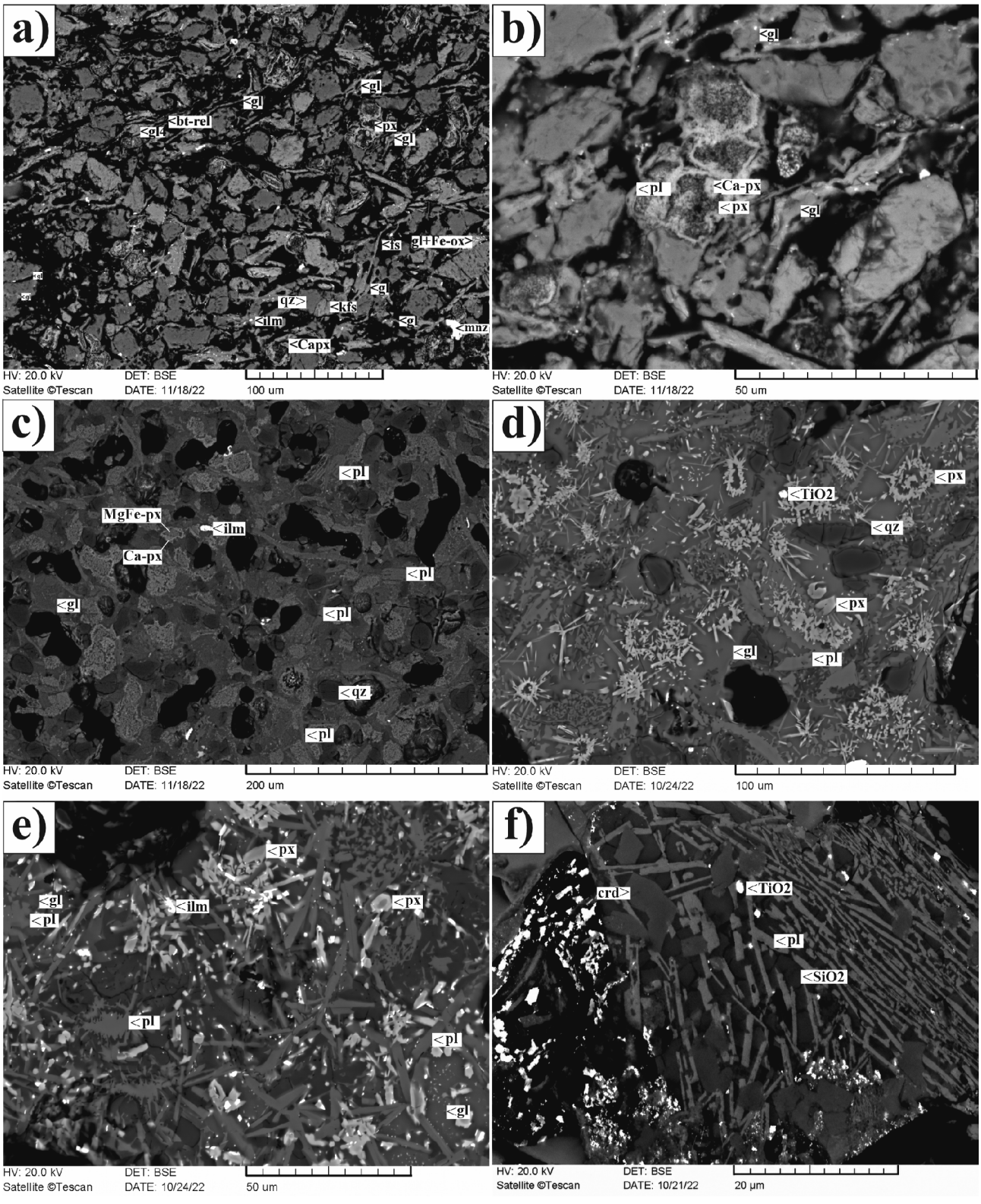


Figure 4. Backscattered electron image of rock samples from the Rónabánya Combustion Metamorphic Complex a) Relict sedimentary, blastoclastic texture of clinker sample; b) 1-5 µm pyroxene crystallites grouped into 20 µm zoned nodules - shaped like pseudomorphs in clinker; c) Ca-Fe zoned piroxene nodules in hyalopilitic buchite sample; d) spherical-cocarde-like piroxene nodules in hyalopilitic buchite; e) buchite domain with intersertal texture f) intersertal-spinifex texture of paralava sample, Abbreviations: bt - biotite, px - pyroxene, kfs - K-feldspar, ilm - ilmenite, Ca-px - clinopyroxene, qz - quartz, pl - plagioclase, crd - cordierite, gl - glass, mnz - monazite, rel - relict, chemical elements are abbreviated as in periodic table.

4. ábra. *a) Klinker minta relikt üledékes, blasztoklasztos szövete; b) 20 µm-es zónás gumókba rendeződő, 1-5 µm-es piroxén krisztallitok - pszeudomorfőzák formájában a klinkerben; c) Ca-Fe zónás piroxéngumók hialopilites buchit mintában; d) Gömbös, kokárdaszerű piroxéngumók hialopilites buchitban; e) Interszertális szövetű buchit-domén; f) Paraláva minta interszertális-spinifex szövete. Rövidítések: bt - biotit, px - piroxén, kfs - kálifeldpát, ilm - ilmenit, Ca-px - klinopiroxén (Ca-piroxén), qz - kvarc, pl - plagioklász, crd - cordierit, gl - kőzetüveg, mnz - monacit, rel - reliktum; a kémiai elemek rövidítései a periódusos rendszernek felelnek meg.*

few metres and only the fragmented clinker units – sometimes merged with buchite – are visible.

The least metamorphosed rocks are the "clinker" metaaleurolites. In these rocks, the first sign of alteration is the OH-loss of the phyllosilicates (Clark & Peacor 1992) often followed by oxide replacement of Fe-bearing phyllosilicates (*Fig. 4a-b*). Less often mica gets partially melted – indicating an even higher temperature range. This also correlates well with the increasingly frequent cracking in relict quartz crystals in clinker samples with increasing temperature, which is the result of volume changes due to thermal expansion (Ackermann & Sorrell 1974, Clark & Peacor 1992, Di Febo et al. 2020). At unknown temperatures, pyroxene, Ca-rich plagioclase and ilmenite also appear in the clinkers together with <1% pockets of glass in the rock matrix, in which pyroxene appears as zoned pseudomorph aggregates of crystallites, apparently formed from an original (sedimentary) phase, probably by recrystallisation (*Fig. 4c*) (Grapes et al. 2009). With the appearance of pyroxene, the original cement material and the phyllosilicates also transform into ilmenite grains and to glassy material, resulting in a completely ceramic-like texture in the most altered metaaleurolite. The relict detrital quartz in buchites is not only cracked but shows variously intensive resorption at the margins and along the cracks, too. Plagioclase crystals are often symplectitic but also occur in strongly elongated idiomorphic forms. In the case of pyroxene crystals, the rosette-like appearance of the zonal and sub-angular pseudomorphs indicates that the rock was solidified during sudden cooling. Abrupt cooling is also indicated by the concentric, ring-like cracks that appear in the glassy material around relict quartz crystals (Grapes 2011, Di Febo et al. 2020).

With increasing temperature, the appearance and volume of cavities in the rocks also changes: in rocks with few cavities, first angular and then sinusoidal pores appear in place of the original minerals (e.g., biotite; *Fig. 4a-b*), and then, in the transition to buchites the cavities become rounded or spherical (*Fig. 4c-d*) which was also observed by Grapes et al. (2009). The persistently higher temperatures of the upward flowing and igniting possibly reductive 'gas flares' may have resulted in high grade melting of the rock, and the combination of gas-rich melt and continued gas upwelling may have allowed the formation of slag-like, extremely vesicular lavas. The degree of metamorphism in these rocks is no longer meaningfully discussed, as the minerals in the rocks have crystallised from melt.

Formation temperature

For the metaaleurolite formation temperatures above 550 °C can be estimated on the loss of OH in phyllosilicates (Földvári 1986). To give estimation on the formation temperature of buchite and paralava without complex calculations, and knowing the fact that the temperature during alteration was presumably increasing rapidly in the burning environment consequently propagating metastable mineral transitions – we decided to use natural and industrial analogues. The morphology, the needle or plate-like SiO_2 crystals (cristobalte+tridymite) that appear in both buchite and paralava indicate that the rocks may have been formed at temperatures above 900 °C (Cole 1935, Di Febo et al. 2020). However, this estimate is also dependent on the composition of the fluids present in the system. The formation temperature above 900 °C of buchite and paralava may also be indicated by cristobalite crystallising directly incubating from quartz and from the melt, but quartz did not form crystallizing from melt (Cole 1935). Although cristobalite and tridymite crystals are not clearly distinguishable in thin section the morphology is dominated by well-developed needle and plate like elongated crystals matching the morphological features of cristobalite described by Di Febo et al. (2020). The retrograde temperature regimes also described by Cole (1935) may result in the formation of tridymite as retrograde mineralogy from cristobalite. These observations altogether would suggest primary cristobalite formation with minor tridymite probably present and late stage retrograde tridymite formation. That also explains the relatively lower intensity/or least definitive peaks of tridymite present in the highest temperature rock assemblages (Suppl. 1A.).

Cosca et al. (1989) estimated minimum formation temperatures of 1020-1400 °C for paralavas associated with natural coal fires in the Powder River Basin. Furthermore, paralavas from other natural coal fires, such as those in the Most Basin (Czechia), reflect a similarly broad formation range up to 1450 °C. The mineral assemblage we found in the buchite and paralava rocks is similar to the one identified by Grapes et al. (2009). The combustion metamorphic complex described in this study has a resemblance with the RCMC, by not only the geological setting or the protolith, but the described anorthite-pyroxene-cordierite-Fe-Ti-oxide-glass assemblage they found in natural paralava. They estimated liquidus temperatures between 1120 and 1230 °C for the paralava. In industrial slags and ceramics (where metastable mineral formation and abrupt cooling are also key factors of mineral formation) the plagioclase-pyroxene-cordierite assemblage yield an estimated temperature of ~1250 °C (Shu et al. 2015), whereas the plagioclase-cristobalite assemblage suggests 1200-1225 °C (Taskiran et al. 2005). Taking these natural and industrial analogues into consideration a maximum formation temperature range of 1100-1200 °C can be roughly estimated for the complex presented in our study based on the mineral assemblage found in paralava.

The heat required for the formation of the complex could have been supplied by the oxidation and burnout of the upper coal bed of the Salgótarján Brown Coal Formation III. coal deposit (*Fig. 1c*). Based on the size and location of the coal seams and the burnt-out coal seams in the upper layer, it can be stated that the original sedimentary layers and the altered layers correlate well. Regarding our field observations, these coal seams are now only visible as layers of pure, grey-white laminated amorphous SiO_2, with opalised plant remains. The sedimentary rocks deposited over the coal seams were altered by the heat to the clinker and buchite units seen today.

Origin and temporality of the complex

The currently visible, actual extent of the metamorphic complex indicates that the formations were clearly exposed to subrecent erosion, as the altered rocks are consistently found in the sediments of a landslide few hundred meters away from the studied outcrop. Considering the known periods of mining, as well as the quantity and extent of the rocks occurring in the landslide, the landslide can be considered as the result of pre-mining erosion. Thus, overall, the natural origin of the complex is a viable consideration; however, based on the available literature discussed earlier and fundamentally the lack of data regarding the landslide's exact age, its anthropogenic nature cannot be ruled out either.

Conclusion

The zonation of the rocks encountered in the outcrop, the macroscopic texture, mineral composition and petrographic analysis of the samples collected allowed the petrogenetic interpretation that a yet undescribed combustion metamorphic complex is located in the Salgótarján Basin, near Rónabánya village. In the studied outcrops we could observe almost all the outcrop-scale formations associated with siliciclastic combustion metamorphic features: the highest-temperature zone in the core of the complex, the 'chimney structure'; the surrounding fractured, partially melted rocks, buchites; and the surrounding metaaleurolites – clinkers at a distance of several 10 m. The zonation in the altered rocks continues eastwards from the chimney structure for 200 metres, where it reaches the original aleurolite, which has not been significantly affected by heat. The complexity, the preservation, and the connection to some already protected geosites makes this an exceptional new preservation locality in the Geopark.

Based on the mineral assemblages of the altered rocks the following formation temperature estimates can be given: clinker–metaaleurolite above ~550 °C based on the gradual loss of OH in the phyllosilicate phases, the appearance of pyroxene and the texture of quartz grains indicating volume change; buchite above 900 °C due to metastable SiO_2 – cristobalite and tridymite – formation; paralava ~1100-1200 °C based on the anorthite-pyroxene-cordierite-Fe-Ti-oxide-glass assemblage. These temperature data are consistent with formation temperatures documented in foreign natural analogues and industrial slags and ceramics. For some parts of the complex the actual temperature is presumably lower than these estimated values due to the presence of volatiles in the system.

Acknowledgement

This research was initiated following the idea and guidance of our professor and mentor, Dr. Tamás WEISZBURG, whose support and mentorship were instrumental in launching and developing this study. We would like to express our sincere gratitude to him for introducing the research topic and for his continuous guidance throughout the work.

This study was supported by the New National Excellence Program (ÚNKP – Új Nemzeti Kiválósági Program) of the National Research, Development and Innovation Office of Hungary given to L. HORVÁTH (*ÚNKP-23-2-II-ELTE-124*). The authors would like to thank the anonymous reviewer for their hard work, thorough review, and dedicated attention to our manuscript. We gratefully acknowledge the Institute of Geography and Earth Sciences, Department of Mineralogy, Eötvös Loránd University, for providing the instrumental background necessary for this research. We specially thank Sándor VÁGÓ, Tamás GHERDÁN and Zita BORBÁS for providing field support. We also sincerely thank the staff of the Novohrad–Nógrád UNESCO Global Geopark for their valuable assistance and support.

References – Irodalom

ACKERMANN, R. J. & SORRELL, C. A. 1974: Thermal expansion and the high–low transformation in quartz. I. High-temperature X-ray studies. – *Journal of Applied Crystallography* **7/5,** 461–467. https://doi.org/10.1107/S0021889874010211

ANDERSEN, O. 1915: The System Anorthite-Forsterite-Silica. – *American Journal of Science*, s4-39(232), 407–454. https://doi.org/10.2475/AJS.S4-39.232.407

BENTOR, Y. K., KASTNER, M., PERLMAN, I. & YELLIN, Y. 1981: Combustion metamorphism of bituminous sediments and the formation of melts of granitic and sedimentary composition. – *Geochimica et Cosmochimica Acta* **45,** 2229–2255.

CIESIELCZUK, J., KRUSZEWSKI, Ł. & MAJKA, J. 2015a: Comparative mineralogical study of thermally-altered coal-dump waste, natural rocks and the products of laboratory heating experiments. – *International Journal of Coal Geology* **139/1,** 114–141. https://doi.org/10.1016/j.coal.2014.08.013

CIESIELCZUK, J., BZOWSKA, G. & PASZKOWSKI, M. 2015b: Mineral Transformations and Actinide Transport: Combustion Metamorphism in the Wojkowice Coal-Waste Dump, Upper Silesian Coal Basin, Poland. – In: *Coal and Peat Fires: A Global Perspective* **3,** 476–491, Elsevier Inc. https://doi.org/10.1016/B978-0-444-59509-6.00017-X

Clark, B. H. & Peacor, D. R. 1992: Pyrometamorphism and partial melting of shales during combustion metamorphism: mineralogical, textural, and chemical effects. – In: *Contributions to Mineralogy and Petrology* **112,** 558–568. https://doi.org/10.1007/BF00310784

Cole, S. 1935: The conversion of quartz into cristobalite below 1000°C, and some properties of the cristobalite formed. – *Journal of the American Ceramic Society* **18/1–12,** 149–154. https://doi.org/10.1111/J.1151-2916.1935.TB19371.X

Cosca, A. M., Essene, E. J., Geissman, J. W., Simmons, W. B. & Coates, D. A. 1989: Pyrometamorphic rocks associated with naturally burned coal beds, Powder River Basin, Wyoming. – *American Mineralogist* **74,** 85–100.

Di Febo, R., Casas, L., del Campo, Á. A., Rius, J., Vallcorba, O., Melgarejo, J. C. & Capelli, C. 2020: Recognizing and understanding silica-polymorph microcrystals in ceramic glazes. – *Journal of the European Ceramic Society* **40/15,** 6188–6199. https://doi.org/10.1016/J.JEURCERAMSOC.2020.05.063

Dzsida J. 1944: *A Salgótarjáni Kőszénbánya R. T. nógrádi szénbányászatának története 1868–1943-ig.* – A Salgótarjáni Kőszénbánya Rt. Igazgatósága.

Földvári M. 1986: *A földtani kutatásban alkalmazott termoanalitikai módszerek*. – Magyar Állami Földtani Intézet.

Grapes, R. 2011: *Pyrometamorphism.* – Second Edition, Springer-Verlag Berlin Heidelberg. https://doi.org/10.1007/978-3-642-15588-8

Gross, S. 1977: The mineralogy of the Hatrurim Formation, Israel. – *Geol. Surv. Israel, Bull.,* **70,** 1–80.

Gupta, T. K. & Jean, J.-H. 1994: Origin of cristobalite formation during sintering of a binary mixture of borosilicate glass and high silica glass. – *Journal of Materials Research* **9/4,** 999–1005. http://journals.cambridge.org

Heffern, E. L. & Coates, D. 2004: Geologic history of natural coal-bed fires, Powder River basin, USA. – *International Journal of Coal Geology* **59/1–2,** 25–47. https://doi.org/10.1016/j.coal.2003.07.002

Kercsmár Zs. & Budai T. 2015: *Magyarország felszíni képződményeinek földtana magyarázó Magyarország földtani térképéhez (1:500 000).* – Magyar Földtani és Geofizikai Intézet.

Laita, E., Bauluz, B. & Yuste, A. 2019: High-temperature mineral phases generated in natural clinkers by spontaneous combustion of coal. – *Minerals* **9/4**. https://doi.org/10.3390/min9040213

Lukács, R., Harangi, S., Guillong, M., Bachmann, O., Fodor, L., Buret, Y., Dunkl, I., Sliwinski, J., von Quadt, A., Peytcheva, I. & Zimmerer, M. 2018: Early to Mid-Miocene syn-extensional massive silicic volcanism in the Pannonian Basin (East-Central Europe): Eruption chronology, correlation potential and geodynamic implications. – *Earth-Science Reviews* **179,** 1–19. https://doi.org/10.1016/J.EARSCIREV.2018.02.005

Misra, B. K. & Singh, B. D. 1994: Susceptibility to spontaneous combustion of Indian coals and lignites: an organic petrographic autopsy. – *International Journal of Coal Geology* **25,** 265–286. https://doi.org/10.1016/0166-5162(94)90019-1

Nawrocki, J., Ciesielczuk, J., Jura, D., Fabiańska, M. J. & Misz-Kennan, M. 2022: The Miocene deep- seated spontaneous coal- seam fire in the Upper Silesian Coal Basin (S Poland) and its geotectonic trigger mechanism. – *Terra Nova* **34,** 184–192. https://doi.org/10.1111/ter.12576

Noszky J., ifj. 1931: *Salgótarján és barnakőszén-bányászata, különös tekintettel a néprajzi viszonyokra.* – Rudabánya, 2007.

Pagliari, L., Dapiaggi, M., Pavese, A. & Francescon, F. 2013: A kinetic study of the quartz-cristobalite phase transition. – *Journal of the European Ceramic Society* **33/15–16,** 3403–3410. https://doi.org/10.1016/j.jeurceramsoc.2013.06.014

Radócz G., Hámor G. & Selmeczi I. 2023: *Magyarország litosztratigráfiai egységeinek leírása II. Kainozoos képződmények.* – Szabályozott Tevékenységek Felügyeleti Hatósága.

Shu, Q., Wang, Y., Li, J., Liu, Y., Li, P. & Chou, K. 2015: Effect of Na2O on dissolution rate of alumina in CaO-Al2O3-MgO-SiO2 slag. – *ISIJ International* **55/11,** 2297–2303. https://doi.org/10.2355/isijinternational.ISIJINT-2015-211

Sokol, E. V. & Volkova, N. I. 2007: Combustion metamorphic events resulting from natural coal fires. – *Reviews in Engineering Geology* **18**. https://doi.org/10.1130/2007.4118(07)

Stracher, G. B. & Taylor, T. P. 2004: Coal fires burning out of control around the world: Thermodynamic recipe for environmental catastrophe. – *International Journal of Coal Geology* **59/1–2,** 7–17. https://doi.org/10.1016/j.coal.2003.03.002

Taskiran, M. U., Demirkol, N. & Capoglu, A. 2005: A new porcelainised stoneware material based on anorthite. – *Journal of the European Ceramic Society* **25/4,** 293–300. https://doi.org/10.1016/j.jeurceramsoc.2004.03.017

Žáček, V. & Skála, R. 2015: Mineralogy of Burning-Coal Waste Piles in Collieries of the Czech Republic. – In: *Coal and Peat Fires: A Global Perspective* **3,** 110–159, Elsevier Inc. https://doi.org/10.1016/B978-0-444-59509-6.00005-3

Žáček, V., Skála, R., Chlupáčová, M. & Dvořák, Z. 2005: Ca-Fe3+-rich, Si-undersaturated buchite from Zelenky, North-Bohemian Brown Coal Basin, Czech Republic. – *European Journal of Mineralogy* **17/4,** 623–634. https://doi.org/10.1127/0935-1221/2005/0017-0623

Žáček, V., Skála, R. & Dvořák, Z. 2015: Combustion Metamorphism in the Most Basin, Czech Republic. – In *Coal and Peat Fires: A Global Perspective* **3,** 162–202, Elsevier Inc. https://doi.org/10.1016/B978-0-444-59509-6.00006-5

Manuscript received: 2026/08/25

Supplementary Materials

Table SM 1A. Results of the XRD measurements
SM 1A táblázat. *XRD-mérések eredményei*

Metaaleurolite			Buchite			Buchite			Paralava			Paralava		
d value (Å)	Int. (%)	Mineral	d value (Å)	Int. (%)	Mineral	d value (Å)	Int. (%)	Mineral	d value (Å)	Int. (%)	Mineral	d value (Å)	Int. (%)	Mineral
10.0	12	Bt	8.5	18.3	Crd	4.68	20.6	Trd	8.6	15.3	Fs	8.5	43	Crd
9.7	6.1		6.5	12.9	An	4.57	27.6	Fs	8.2	17.3	Crd	7.4	9.4	
6.4	3.4	Ab	5.1	12		4.35	22.5	Trd	6.5	17.4	An	6.5	10.2	An
5.8	2.7	Ab	4.90	14.3	Crd	4.25	36.7	Qz	4.72	21.5	An	6.1	9.3	
5.6	2.4	Ab	4.68	14	Crd	4.07	76	Crs	4.65	19.1	Crd	5.5	9.5	
5.0	8.3	Ilt	4.56	12.7	Trd	4.05	65	Crs, An	4.57	21.3	Fs	5.3	9.3	
4.67	3.2		4.33	18.6	Trd	3.91	24.5	An	4.33	36.8	Trd	4.88	14.1	Crd
4.49	8.6	Ilt	4.26	28.5	Qz	3.76	28.6	An	4.26	26.2	Qz	4.67	13.6	Crd
4.25	22.5	Qz	4.08	56.2	An, Crd, Crs	3.63	24.9	An	4.06	100	An, Crd, Crs	4.54	11.8	Trd
4.03	5.7	Ab	3.90	18.3	Trd	3.45	19.7	An	3.96	21.7	An	4.32	17.8	Trd
3.91	4.4	Ab	3.76	24.9	An	3.34	100	Qz, An, Fs	3.90	28	Trd	4.09	100	An, Crd
3.78	5.1	Ab	3.63	18.3	An	3.24	26.8	An	3.76	31.8	An	3.76	17.5	An
3.69	3.4	Ab	3.55	13.4	An	3.19	84.2	An, Fs	3.63	26.9	An, Fs	3.64	13.9	An
3.51	5.4	Ilt	3.47	15	An	3.13	29.3	An	3.42	20.2	An, Fs	3.47	12.1	An
3.34	100	Qz, Ilt, Bt	3.34	100	An, Fs, Crd, Qz	3.02	23	An	3.34	41.9	An, Fs, Crd, Qz	3.37	28.3	Crd
3.22	7.5	Ab, Ilt	3.24	21.6	An, Trd	2.95688	27.4	Fs, Trd, An	3.23	30.8	An	3.35	21.3	Qz
3.19	9.8		3.19	50.7	An, Fs	2.88287	34	Fs	3.18	70.4	An, Fs	3.24	16.5	An
3.03	3.7	Cal	3.14	21	Crd, Trd, Crs	2.83602	24.7	An, Fs, Crs	3.13	32.4	An, Crd	3.19	28.7	An
2.96119	3.1	Ilt	3.00	17.8	Crd	2.77352	14.9		3.02	21.2	An, Crd	3.14	34.4	An, Crd,
2.92938	3.2	Bt	2.94742	18.9	Fs, Trd	2.74433	15.1		2.95051	26.9	An, Fs, Trd	3.03	32	Crd
2.87786	3.6	Ilt	2.88014	20.1	An, Fs	2.72378	16	Fs	2.88104	29.2	An, Fs	2.82794	11.1	An
2.64266	3.1	Ab	2.83224	15.4	An, Fs, Crs	2.64599	16.3	An	2.83520	25.7	An, Fs	2.64456	12.7	An, Crd
2.59353	4.3	Ilt	2.65360	11.6	An, Crd	2.55203	20.2	Fs	2.71400	16.6	An, Fs	2.51127	23.8	An
2.51079	4.8	Bt, Ilt	2.56384	13.9	An	2.51124	31.9	An, Fs, Crs	2.65360	16.9	An, Crd	2.49654	19.1	Trd
2.45362	8.3	Qz	2.54096	15.7	Fs	2.47943	25.6	An	2.57165	13.8	Fs, Trd	2.44322	9	An
2.40066	3	Ab, Ilt	2.51113	22.5	An	2.45430	19.6	Qz	2.54104	21.5	Fs	2.33263	8.6	Crd
2.31590	3	Ab	2.45633	15.8	Crd	2.40531	14.4	An, Fs	2.50834	41.2	An, Fs, Trd	2.30677	7.1	An
2.28119	7.5	Qz	2.41537	11.5	Crd	2.38684	13	An	2.41960	15	Crd	2.28015	8.2	Crd
2.23600	4.3	Qz	2.38720	9.7	An	2.28215	14.1	Qz	2.27480	14.2	An, Fs	2.16072	7.5	Qz
2.15292	2.9	Ab, Ilt	2.28055	13.7	Qz, Crd	2.23349	15.3	An	2.15680	11.6	An, Crd	2.13281	10.5	An, Qz
2.12706	6	Qz	2.23639	10.7	An, Qz, Crd	2.15867	13.7	An	2.13145	21.2	An, Fs	2.09844	10.4	An, Crd, Trd
2.00702	4.4	Ilt, Bt	2.18430	8.7	An	2.12832	21.8	Crs, An	2.09778	17.9	An, Crd, Trd	2.04594	8.5	Crd
1.97948	4	Qz	2.12877	15.1	An, Qz, Trd, Fs	2.10744	17	Fs	2.05407	12.2	Fs, Trd	2.00708	7.1	An
1.81657	10.4	Qz	2.02719	9.2	An, Fs	2.03148	12.7	Trd	2.02552	14.3	An, Trd	1.98880	6.8	An
1.67048	4.7	Qz	1.98195	10.4	An, Fs	2.01761	11.1	An	1.98779	14.7	An, Fs	1.87974	9.8	An
1.65973	3.1	Qz	1.92729	10.1	An, Fs	1.99817	13.9	Fs	1.92779	13.2	An, Fs	1.81661	7.9	An
1.54106	6.5	Qz	1.84299	10.1	Crd	1.96845	12.5	Fs	1.84176	13	Crd	1.79515	8.2	An
			1.81664	15.8	Qz	1.93373	11.5	Crs, An	1.81813	13	Qz	1.77201	8.3	An
			1.79815	9.6	An, Crd	1.81597	16.6	Qz	1.79673	12.1	An, Crd	1.71509	8	An
			1.77368	9.3	An	1.76821	13.9	An, Fs	1.77077	14.7	An	1.69030	12.1	Crd
			1.74464	8.3	An	1.74772	13.6	Fs	1.72636	12.4	Fs	1.67752	6.1	Qz
			1.71128	9.2	An, Fs	1.62174	15.8	Fs	1.70708	13	Crd	1.62349	8.8	An
			1.68523	8	Crd	1.59445	12	Fs	1.61748	16.6	Crd	1.57161	7.1	An
			1.67382	8.5	Qz, Fs	1.56815	9.8		1.60265	11.6	Fs	1.52594	6.5	An
			1.62744	10.5	Fs	1.54880	11.3		1.59407	10.6	An	1.45534	7.6	An, Crd
			1.54000	12.1	An, Qz	1.54149	15.6	Qz	1.57882	10.3	An	1.44856	8.7	An
			1.47240	8.9	An, Fs	1.52653	12.2	Fs, Trd	1.57007	10.4	An			
			1.45537	8.9		1.49161	16.1	Fs	1.55714	11.4	Crd			
									1.54243	15.3	An, Qz			
									1.52310	10.9	Crd			
									1.48974	15	Fs, Crd			

Table SM 1B. Results of semi-quantitative measurements of glass and rock-forming minerals.
Abbreviations: CS=metaaleurolite, B=buchite, PL=paralava.

SM 1B táblázat. *A kőzetüveg és a kőzetalkotó ásványok szemikvantitatív méréseinek eredményei.*
Rövidítések: CS=metaaleurolit, B=buchit, PL=paraláva.

a) Glass

ID / oxide wt%	SiO_2	TiO_2	Al_2O_3	Fe_2O_3	MnO	MgO	CaO	Na_2O	K_2O	P_2O_5	TOTAL
CS02_gl1	59,84	0,45	26,09	1,63		3,2	4,21	3,66	0,92		100
CS02_gl2	81,14	0,12	11,84	1,35		2,15	0,88	0,86	1,66		100
CS02_gl3	50,63	0,18	32,1	2,39		6,4	3,71	3,37	1,22		100
CS02_gl4	49,22	0,36	33,48	2,18		4,43	5,7	4,11	0,52		100
B01_red_gl2	69,95		20,42				6,5	2,87	0,27		100
B01_gl_rim	76,15	0,6	14,46	0,76		0,7	2,3	2,3	2,74		100
B01_al_gl	93,79		5,25	0,15					0,81		100
B01_gl0	79	0,42	12,57	0,84		0,79	0,81	1,79	3,78		100
B02_gl1	74,23	0,93	14,03	2	0,14	0,71	0,66	1,48	5,01	0,81	100
B02_gl2	73,95	0,82	13,58	3,11	0,19	0,83	1,15	1,19	4,16	1,03	100
B02_gl3	68,98	0,91	12,06	7,66	0,49	2,03	0,67	1,46	4,52	1,21	100
B02_qz_rim	97,64		2,09	0,27							100
B02_gl4	93,35	0,15	4,32	0,52		0,16	0,2	0,65	0,66		100

b) Cordierite

ID / oxide wt%	SiO_2	TiO_2	Al_2O_3	Fe_2O_3	MgO	Na_2O	CaO	K_2O	TOTAL
PL01_cor1	65,96		23,94	2,61	7,49				100
PL01_cor1_glass	65,14	0,29	23,76	2,58	7,46		0,59	0,18	100
PL01_cor2	55,58		31,49	2,31	10,62				100
PL01_cor2_glass	54,83		31,23	2,27	10,61	0,86		0,21	100

c) Pyroxene

ID / oxide wt%	SiO_2	TiO_2	Al_2O_3	MgO	FeO	MnO	CaO	TOTAL
CS02_capx1	54,11		2,42	20,75	4,01		18,71	100
CS02_capx2	51,89	0,43	4,59	14,77	7,68		20,64	100
CS02_px_rim	53,63		4,68	19,95	4,92		16,82	100
B01_capx	59,39		4	15,15	5,85		15,6	100
B01_ca2px	56,64		7,53	14,45	4,18		17,2	100
B01_px_rim	55,73		3,29	24,83	13,63		2,52	100
B01_px	55,42		3,6	22,42	17,45		1,11	100
B01_px2	57,65		4,53	24,69	12,03		1,1	100
B04_px_inside	54,3	0,42	4,02	25,11	13,49	0,04	2,61	100
B04_px_inside2	55,5	0,35	3,32	26,84	12,36	0,13	1,5	100
B04_px_rim	53,23	0,52	5,89	20,19	16,86		3,32	100

d) Sheet silicates

ID / oxide wt%	SiO_2	TiO_2	Al_2O_3	MgO	FeO	Na_2O	K_2O	TOTAL
CS01_mus	51,15	0,17	31,07	3,75	2,89	0,74	8,23	98
CS03_chl	30,91	1,31	22,52	6,2	33,63	1,97	1,46	98
CS03_chl2	27,84	0,91	27,69	7,58	31,24	1,35	1,39	98
CS03_bt	47,06	2,21	20,44	4,97	20,53	1,25	1,54	98
CS02_sht	51,14	3,08	18,52	11,56	12,94		0,76	98
CS02_bt	51,07	1,43	18,96	13,29	12,6		0,66	98
CS02_Al_rich	31,21	0,41	41,18	14,36	8,71		2,13	98

Table SM 1B. Continued
SM 1B táblázat. *folytatás*

e) Amphibole

ID / oxide wt%	SiO_2	TiO_2	Al_2O_3	MgO	FeO	MnO	CaO	TOTAL
CS01	37,44	0	21,64	3,38	28,08	1,05	6,39	98

f) Feldspar

ID / oxide wt%	SiO_2	Al_2O_3	CaO	Na_2O	K_2O	FeO	TOTAL
CS03_fs1	65,7	23,93	2,66	2,95	3,51	1,25	100
CS03_fs2	67,67	20,14	4,98	3,44	3,06	0,72	100
B01_plag1	56,54	28,58	10,78	1,09	2,26	0,75	100
B01_plag1rim	51,94	31,04	14,1	1,19	0,62	1,12	100
B01_plag2	45,72	35,84	15,41	1,28	0,34	1,41	100
B02_plag1	59,04	26,13	9,16	2,36	2,1	1,22	100
B04_plag1	54,03	28,79	12,27	1,92	1,12	1,87	100
B04_plag2	49,2	32,83	15,11	1,62	0,21	1,02	100
PL01_fs1	60,79	23,45	9,68	2,21	2,42	1,45	100
PL01_plag1	56,14	29,03	13,36	0,97	0,18	0,32	100
PL01_plag2	60,42	25,39	11,85	0,98	0,09	1,27	100